VOL. 13, NO. 17, SEPTEMBER 2018 ISSN 1819-6608
ARPN Journal of Engineering and Applied Sciences


www.arpnjournals.com

# NONLINEAR FLUID MODEL FOR BLOOD RHEOLOGY IN NARROW ARTERIES WITH CONSTRICTION AND DILATATION

D. S. Sankar
School of Applied Sciences and Mathematics, UniversitiTeknologi Brunei, JalanTungku Link, Gadong, BA1410, Brunei Darussalam
E-Mail: duraisamy.sankar@itb.edu.bn

## ABSTRACT

This theoretical model mathematically analyses the steady flow of blood in a tapered narrow artery with mild stenosis and dilation, treating the blood as non-Newtonian Casson fluid model. The resulting nonlinear boundary value problem is solved to obtain the analytic expressions to the velocity profile, volumetric flow rate, pressure gradient, wall shear stress and longitudinal impedance to flow. The influence of various flow parameters on the aforesaid rheological quantities are analyzed through appropriate graphical and tabular representation of data. It is noted that the pressure gradient and wall shear stress increases with the increase of the maximum depth of stenosis, yield stress and consistency index of blood and, it decreases with the increase of the angle of tapering, flow rate and maximum height of dilatation. It is also found that the blood velocity decreases considerably with the increase of the yield stress of blood and it decreases significantly with the increase of the consistency index. The percentage of increase in the frictional resistance to flow increases rapidly with the increase of the maximum depth of stenosis and maximum height of dilatation and, it increases marginally with the increase of the yield stress of blood.

**Keywords:** steady flow, casson fluid, axi-symmetric stenosiss, dilatation, frictional resistance.

## INTRODUCTION

Blood vessels' wall is hardened and the blood passage region is constricted by the development of atherosclerotic plaques which are technically called as stenosis and are formed by the deposit of fats, lipids, cholesterol and other unsaturated substances in the lumen of arteries [1-3]. When the stenosis grows in an artery, it considerably affects the normal blood circulation, changes the blood flow pattern and thus it significantly enhances the wall shear stress and resistance to flow and thus, it leads to many cardiovascular diseases like heart attack, ischemia strokes like cardiac ischemia, brain ischemia, etc. which claim the life of millions of people around the world every year [4 - 6]. The serious consequences of arterial stenosis draw the attention of several researchers to find the chemical, biological and fluid dynamical factors which influence the development of arterial stenosis [7 - 11]. Tang *et al*. [12] reported that the continuous development of stenosis may damage the cells in the lumen of the artery and the arterial segment with stenosis may be collapsed due to the low pressure which causes severe blood pooling in that locality. Thus, it is important to analyze the influence of arterial stenosis on the fluid dynamical characteristics of blood.

Vasodilatation is the biological process of widening of blood vessels which is caused by relaxation of smooth muscle cells on the inner wall of smaller and larger diameter blood vessels [13] and is opposite to the process of vasoconstriction. The development of dilation in blood vessels increases the blood flow and thus it decreases the resistance to flow [14]. Since the dilation in arteries and arterioles reduces arterial blood pressure and heart rate, artificial artery dilators are used to treat heart failure, systemic and pulmonary hypertension, and angina [15]. Vasodilation occurs in arterioles when the tissues are not receiving enough glucose or lipids or other nutrients [16]. Vasodilators are the factors that results in vasodilation and some of them are carbondioxide and Nitric oxide [17, 18]. Hence, it is useful to investigate the effects of vasodilation on the rheological properties of blood.

It has been well established that blood behaves like Newtonian fluid when it flows in larger diameter arteries ($>1300\,\mu m$) at high shear rates ($>100/s$), but when it flows through smaller diameter arteries ($50-1300\,\mu m$) at low shear stress ($<100/s$), it exhibits remarkable non-Newtonian fluids' character [19, 20]. Several researchers attempted to analyze the blood rheology when it flows through smaller diameter arteries at low shear rates under normal (tapered, non-tapered etc) and abnormal (stenosis, aneurysm, stented, catheterizedetc) conditions, treating blood as non-Newtonian fluid model with or without yield stress and pointed out the effects of abnormal conditions on blood flow characteristics [21 - 25].

Casson fluid model is a non-Newtonian fluid (non-linear) model with yield stress which is widely applied in the mathematical modeling of blood rheology in narrow arteries [26]. Casson [27] investigated *in vivo* the appropriateness of Casson fluid for modeling blood and propounded that at low shear rates, the yield stress value of blood is nonzero. Scott Blair [28] propounded that the Casson fluid's parameters such as viscosity and yield stress are adequate to describe the shear flow of blood. Merrill *et al*. [29] reported that Casson fluid's constitutive lawholds good for blood flow in arteries of diameter $130\mu m$ - 1300 $\mu m$. Scott Blair and Spanner [30] pointed out that blood behaves like a Casson fluid when it flows in small diameter arteries at moderate shear rates. Hence, it is more appropriate to assume blood as a Casson fluid when it flows through narrow arteries at low shear rates.

Several attempts were made by researchers to study the non-Newtonian behavior of blood when it flows

in smaller diameter arteries, treating blood as Casson fluid [31 - 33]. Pincombe *et al*. [34] studied the fully developed flow of Caason fluid through a non-tapered narrow artery in the presence of stenosis and dilatation and obtained analytical solutions to flow rate and resistance to flow. Priyadharshini and Ponnalagusamy [35] analyzed the steady flow of blood through a narrow artery with constriction and dilation, treating blood as Herschel-Bulkley fluid. It is aimed to develop amathematical model to analyze the steady, laminar, axi-symmetric and fully developed flow of blood through a tapered narrow artery with mild stenosis and mild dilation, treating the blood as non-Newtonian Casson fluid.

Though the formulation and solution method of the present study looks similar to that of Pincombe *et al*. [34] (both studies primarily use Casson fluid model for blood flow through arteries with constriction and dilatation), our proposed study differs significantly from their studies and these differences are spelt out below:

a) The tapering of the arterial segment is incorporated in this study which was not considered in their studies.
b) Two different methods are used (analytical and numerical) to find out and verify the pressure gradient which are different from their method.
c) The expressions for velocity distribution, wall shear stress and stream function are obtained in the present works which are not dealt in their studies.
d) The expression obtained for flow rate and resistance to flow are different from the corresponding expressions obtained by them.
e) The results and discussion section of this study discusses the variations of several parameters on the rheological quantities such as pressure gradient, velocity profiles, wall shear stress, resistance to flow and stream lines pattern and these are not analyzed in their studies.

Since, the proposed study is quite different from the studies of Pincombe *et al*. [34] and the aforesaid differences in the studies of blood flow was not investigated by any researcher so far, it is aimed to study the steady, laminar, axi-symmetric and fully developed flow of blood in a narrow artery with mild stenosis and dilatation, treating the blood as Casson fluid. This paper is organized as briefed below:

Section 2 formulates the physical problem mathematically and then the non-dimensional form of the governing equations is obtained. In Section 3, the resulting non-linear boundary value problem is solved along with the set of boundary conditions. The influence of various rheological parameters on the important flow measurements are discussed in the results and discussion Section 4. Section 5 collates the major outcomes of this mathematical analysis.

## MATHEMATICAL MODEL

### Governing equations

Let us consider the steady, axially symmetric, laminar and fully developed flow of blood in the axial direction through atapered narrow artery with stenosis and dilatation, treating blood as viscous incompressible fluid and is modeled as non-Newtonian Casson fluid. The stenosis and dilatation in the artery are considered to be mild and axially symmetric. Two dimensional view of the segment of atapered narrow artery with stenosis and dilatation is depicted in Figure-1a. We have used the cylindrical polar coordinate system $\left(\bar{r},\bar{\theta},\bar{z}\right)$ to mathematically analyze the flow pattern, where $\bar{r}$ and $\bar{z}$ are the coordinates in the radial and axial directions respectively and $\bar{\theta}$ is the azimuthal angle. The mathematical representation of segment of atapered artery with stenosis and dilatationis defined as

$$\bar{R}\left(\bar{z}\right)=\begin{cases}\left(\bar{R}_0-\zeta\bar{z}\right)\bar{A}\left(\bar{z}\right), & \text{if } \bar{\alpha}_i\le\bar{z}\le\bar{\beta}_i\\ \left(\bar{R}_0-\zeta\bar{z}\right), & \text{otherwise}\end{cases} \tag{1a}$$

where

$$\bar{A}\left(\bar{z}\right)=\left[1-\frac{\bar{\delta}_i}{2\bar{R}_0}\left\{1+\cos\left[\frac{2\pi}{\bar{l}_i}\left(\bar{z}-\bar{\alpha}_i-\frac{\bar{l}_i}{2}\right)\right]\right\}\right], \tag{1b}$$

$\bar{\delta}_i$ denotes the maximum projection (depth/height) of the $i^{th}$ abnormal segment into the lumen and it is positive for stenosis and negative for dilatation (aneurysms), $\bar{R}_0$ is the radius of the normal artery, $\bar{R}\left(\bar{z}\right)$ is the radius of the artery in the abnormal (stenosis/aneurysm) region, $\zeta=\tan\psi$, $\psi$ is the angle of tapering of the artery, $\bar{l}_i$ is the length of $i^{th}$ abnormal segment of the artery, $\bar{\alpha}_i$ is the distance of the starting point of $i^{th}$ abnormal segment from the origin and is defined as

$$\bar{\alpha}_i=\left(\sum_{j=1}^{i}\left(\bar{d}_j+\bar{l}_j\right)-\bar{l}_i\right) \tag{1c}$$

where $\bar{\beta}_i$ is the distance between the origin of the flow region and the end of $i^{th}$ abnormal segment and is defined as

$$\bar{\beta}_i=\sum_{j=1}^{i}\left(\bar{d}_j+\bar{l}_j\right) \tag{1d}$$

where $\bar{d}_i$ is the distance between the end of $(i-1)^{th}$ abnormal segment and start of the $i^{th}$ abnormal segment or from the start of the segment if $i=1$. The geometry of artery for different values of the angle of tapering $\psi$ and for different values of stenosis depth and dilatation height are plotted in Figures-1b and 1c.One can observe that when

the angle of tapering $\psi$ is positive, the artery converges and when it is negative, the artery diverges whereas when it is zero, the artery neither converges nor diverges.

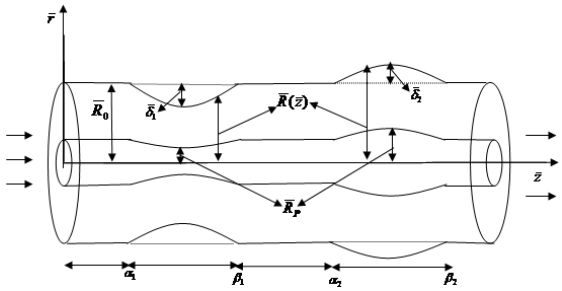


**Figure-1(a).** Geometry of arterial segment with mild stenosis and mild dilatation.

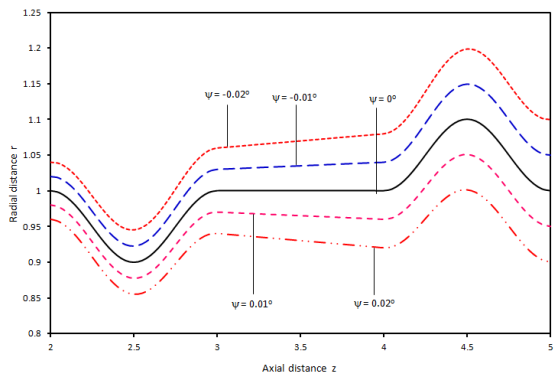


**Figure-1(b).** Geometry of arterial segment for different values of angle of tapering $\psi$with $\delta_1 = 0.1$ and $\delta_2 = -0.1$.

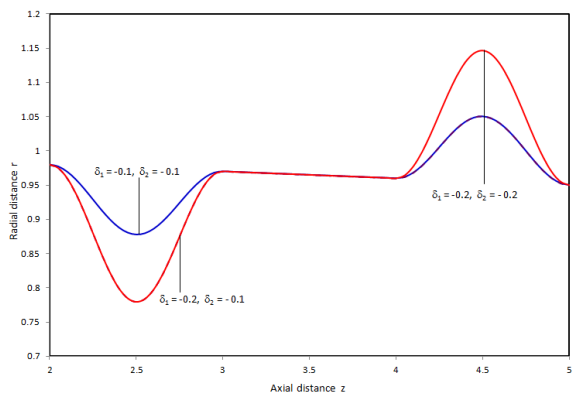


**Figure-1(c).** Geometry of arterial segment for different values of stnosis depth and dilatation height with $\psi = 0.01^{o}$.

The segment of artery under study is assumed to be so long such that the entrance, end and special wall effects are negligibly small in magnitude and thus these are not considered in this study. It is well accepted that for low Reynolds number viscous incompressible fluid flow, the radial component of the velocity is negligibly small and can be ignored. Thus, the axial and radial components of momentum equation governing the blood flow reduce respectively to

$$\frac{\partial \bar{p}}{\partial \bar{z}} = \frac{1}{\bar{r}}\frac{\partial}{\partial \bar{r}}(\bar{r}\,\bar{\tau}); \quad \frac{\partial \bar{p}}{\partial \bar{r}} = 0, \tag{2a; 2b}$$

where $\bar{\tau} = \bar{\tau}_{\bar{r}\bar{z}}$ is the shear stress of blood; $\bar{p}$ is the pressure in the fluid flow; Equation (2b) indicates that the pressure is independent of $\bar{r}$ and it is function of only $\bar{z}$. The simplified form of the constitutive equation of Casson fluid model is [31]

$$-\frac{\partial \bar{u}}{\partial \bar{r}} = \begin{cases} \frac{1}{\bar{k}}\left[\sqrt{\bar{\tau}} - \sqrt{\bar{\tau}_y}\right]^2, & \text{if } \bar{\tau} > \bar{\tau}_y \\ 0 & \text{if } \bar{\tau} \le \bar{\tau}_y \end{cases} \tag{3}$$

where $\bar{u}$, $\bar{\tau}_y$ and $\bar{k}$ are the Casson fluid's axial velocity, yield stress and consistency index respectively. Eq. (3) indicates that normal flow occurs in the region when the shear stress exceed the yield stress and plug flow (solid-like flow) in the region where the shrear stress does not exceed the yield stress limit. When $\bar{\tau}_y = 1$, Equation (3) reduces to the constitutive equation of Newtonian fluid. The boundary conditions appropriate to this flow are

$$\bar{\tau} \text{ is finite and } \bar{r} = 0; \tag{4a}$$

$$\frac{\partial \bar{u}}{\partial \bar{r}} = 0 \;\; at \;\; \bar{r} = 0; \quad \bar{u} = 0 \;\; at \;\; \bar{r} = \bar{R} \tag{4b; 4c}$$

**Non-dimensionalization**

Let us introduce the following non-dimensional variables:

$$R(z) = \bar{R}(\bar{z})/\bar{R}_0;\; z = \bar{z}/\bar{R}_0;\; u = \bar{u}/\bar{u}_0;\; p = \bar{R}_0\bar{p}/\bar{\mu}\bar{u}_0;$$
$$\tau = \bar{R}_0\bar{\tau}/\bar{\mu}\bar{u}_0;\; \tau = \bar{R}_0\bar{\tau}_y/\bar{\mu}\bar{u}_0;\; \delta_i = \bar{\delta}_i/\bar{R}_0;\; l_i = \bar{l}/\bar{R}_0;$$
$$\alpha_i = \bar{\alpha}_i/\bar{R}_0;\; \beta_i = \bar{\beta}_i/\bar{R}_0, \tag{5}$$

where $\bar{u}_0$ is the mean velocity of blood, $\bar{\mu}$ is the coefficient of viscosity of Newtonian fluid. Substitution of the non-dimensional variables in Eqs. (1a) - (1d) yield the mathematical form of geometry of artery in dimensionless form as below respectively:

$$R(z) = \begin{cases} (1-\zeta z)A(z), & \text{if } \alpha_i \le z \le \beta_i \\ (1-\zeta z), & \text{otherwise} \end{cases} \tag{6a}$$

$$A(z) = \left[1 - \frac{\delta_i}{2R_0}\left\{1 + \cos\left[\frac{2\pi}{l_i}\left(z - \alpha_i - \frac{l_i}{2}\right)\right]\right\}\right] \tag{6b}$$

$$\alpha_i = \left(\sum_{j=1}^{i}(d_j + l_j) - l_i\right); \quad \bar{\beta}_i = \sum_{j=1}^{i}(\bar{d}_j + \bar{l}_j). \tag{6b; 6c}$$

Use of the non-dimensional variables into Equations (2a) and (3), we obtain dimensionless form of the momentum and constitutive equations as below:

$$\frac{1}{r}\frac{\partial}{\partial r}(r\tau)=\frac{dp}{dz},\ (7)\ -\frac{\partial u}{\partial r}=\begin{cases}\frac{1}{k}\left[\sqrt{\tau}-\sqrt{\tau_y}\right]^2, & \text{if } \tau>\tau_y\\ 0 & \text{if } \tau\le\tau_y\end{cases}.(8)$$

The dimensionless form of the boundary conditions (4a) - (4c) are

$$\tau \text{ is finite } r=0; \quad (9a)$$

$$\frac{\partial u}{\partial r}=0 \text{ at } r=0; \quad u=0 \ at\ r=R. \quad (9b; 9c)$$

Equations (7) and (8) have to be solved for the shear stress $\tau$ and velocity profile $u$ subject along with the boundary conditions (9a) - (9c).

## METHOD OF SOLUTION

Integrating Equation (7) for shear stress $\tau$ and then making use of boundary condition (10a), we get

$$\tau(r,z)=q(z)r/2\ . \ (10a)$$

where $q(z)=-dp/dz$. From Equation (10a), one can get

$$R_p=2\tau_y/q(z)\ . \quad (10b)$$

Using Equation (10a) in Equation (8) and then making use of Eq. (10b), we obtain the expression for velocity profile as

$$u(r,z)=\left(\frac{R^2q(z)}{2k}\right)$$
$$\times\left[\frac{1}{2}\left\{1-\left(\frac{r}{R}\right)^2\right\}+\left(\frac{R_p}{R}\right)\left\{1-\left(\frac{r}{R}\right)\right\}-\frac{4}{3}\sqrt{\frac{R_p}{R}}\left\{1-\left(\frac{r}{R}\right)^{3/2}\right\}\right] \quad (11)$$

On substituting $r=R_p$ in Equation (11), one can get the velocity in the plug flow region as below:

$$u_p=\left(\frac{R^2q(z)}{4k}\right)\left[1-\frac{8}{3}\sqrt{\frac{R_p}{R}}+2\left(\frac{R_p}{R}\right)-\frac{1}{3}\left(\frac{R_p}{R}\right)^2\right] \quad (12)$$

The stream function $\psi$ is defined in such a way that $u=\partial\psi/\partial r$ and $v=(-1/r)\partial\psi/\partial r$, where $v(r,z)$ the fluid's velocity in the radial direction. Thus the stream function $\psi$ is obtained from the velocity profile and its ultimate expression is given below:

$$\psi(r,z)=\left(\frac{R^4q(z)}{336k}\right)\left(\frac{r}{R}\right)^2$$
$$\times\left[21\left\{4-\left(\frac{r}{R}\right)^2\right\}+28\left(\frac{R_p}{R}\right)\left\{3-2\left(\frac{r}{R}\right)\right\}-16\sqrt{\frac{R_p}{R}}\left\{7-4\left(\frac{r}{R}\right)^{3/2}\right\}\right]. \quad (13)$$

The volumetric flow rate is defined as below:

$$Q=2\int_0^R u(r,z)\ r\ dr=\int_0^{R_p}u_p\ r\ dr+\int_{R_p}^R u(r,z)\ r\ dr. \quad (14)$$

Using Equations (11) and (12) in Eq. (14) and then integrating and simplifying, one can obtain ultimate the expression for the volumetric flow rate as

$$Q(z)=\left(\frac{R^4q(z)}{8k}\right)\left[1-\frac{16}{7}\sqrt{\frac{R_p}{R}}+\frac{4}{3}\left(\frac{R_p}{R}\right)-\frac{1}{21}\left(\frac{R_p}{R}\right)^4\right]. \quad (15)$$

From Equation (15), one can find the pressure gradient in one of the two methods such as (i) Numerical method and (ii) Analytical method and these methods are applied as below:

### Numerical method

Equation (15) can be simplified as an algebraic equation for the pressure gradient $x=q(z)$ as below:

$$x^4-\frac{16\sqrt{2}}{7}\sqrt{\frac{\tau_y}{R}}\,x^{7/2}+\frac{8}{3}\left(\frac{\tau_y}{R}-\frac{3kQ}{R^4}\right)x^3-\frac{16}{21}\left(\frac{\tau_y}{R}\right)^4=0\ . \quad (16)$$

For a given set of values of the parameters $Q,\tau_y$ and $k$, Equation (16) can be solved for the pressure gradient $x=q(z)$ using Newton-Raphson method or similar methods.

### Analytical method

In blood flow through narrow arteries, the yields stress of blood is very small (is in the range of 0 Pa - 0.04 Pa) and in diseased state, its range is 0 Pa - 0.2 Pa[26]. The shear stress at the wall is significantly higher in comparison with the yield stress. Thus, for small values of yield stress, $\tau_y/\tau_w<<1$. On neglecting the terms involving $(\tau_y/\tau_w)^2$ and higher powers of $\tau_y/\tau_w$, Equation (15) can be simplified to the following form:

$$q(z)-\frac{16\sqrt{2}}{7}\sqrt{\frac{\tau_y}{R}}\sqrt{q(z)}+\frac{8}{3}\left(\frac{\tau_y}{R}-\frac{3kQ}{R^4}\right)=0. \quad (17)$$

Equation (17) is solved for $\sqrt{q(z)}$ and then by neglecting the terms involving $(\tau_y/\tau_w)^2$ and higher

powers of $\tau_y/\tau_w$, we obtain the analytic (asymptotic) form of the expression for the pressure gradient as:

$$q(z)=8\left(\frac{Qk}{R^4}\right)+64\sqrt{\frac{Qk\tau_y}{R^7}}+\frac{383}{147}\left(\frac{\tau_y}{R}\right)-32\sqrt{\frac{\tau_y^3}{QkR}} \quad (18)$$

For a given set of values of parameters, one can numerically compute the pressure gradient values from Eq. (16) using Newton-Raphson method and directly from the analytical solution obtained in Equation (18). Table-1 computes the numerical and analytical values of the pressure gradient at different stenosis locations and the difference between these values. The numerical and analytical values of the pressure gradient at different dilatation locations and the difference between these values are computed in Table-2. From Table-1 and Table-2, it is found that the difference between the numerical and analytical values of the pressure gradient is not appreciable. Since the analytical expression of pressure gradient is convenient to apply for obtaining closed form solutions to other physical quantities, we will make use of it to get to the analytical expression for rest of the flow measurements.

**Table-1.** Comparison between the numerical and analytical values of the pressure gradient at different locations of stenotic region of arterial segment with $k = Q = 1$, $\delta_1 = \tau_y = 0.1$ and $\psi = 0.01$.

| z | 2 | 2.1 | 2.2 | 2.3 | 2.4 | 2.5 | 2.6 | 2.7 | 2.8 | 2.9 | 3 |
|---|---|---|---|---|---|---|---|---|---|---|---|
| Numerical Value | 8.0112 | 8.3252 | 9.2222 | 10.5046 | 11.7088 | 12.2146 | 11.7105 | 10.5075 | 9.2261 | 8.3299 | 8.0168 |
| Analytical Value | 8.0115 | 8.3259 | 9.2231 | 10.5057 | 11.71 | 12.2159 | 11.72 | 10.5092 | 9.2275 | 8.331 | 8.0181 |
| Difference | 0.0003 | 0.0007 | 0.0009 | 0.0011 | 0.0012 | 0.0013 | 0.0015 | 0.0017 | 0.0014 | 0.0012 | 0.0013 |

**Table-2.** Comparison between the numerical and analytical values of the pressure gradient at different locations of stenotic region of arterial segment with $k = Q = 1$, $\delta_2 = -0.1$, $\tau_y = 0.1$ and $\psi = 0.01$.

| z | 4 | 4.1 | 4.2 | 4.3 | 4.4 | 4.5 | 4.6 | 4.7 | 4.8 | 4.9 | 5 |
|---|---|---|---|---|---|---|---|---|---|---|---|
| Numerical Value | 8.0224 | 7.7237 | 7.0042 | 6.2267 | 5.6754 | 5.4813 | 5.6762 | 6.2285 | 7.0072 | 7.728 | 8.028 |
| Analytical Value | 8.0231 | 7.7247 | 7.0052 | 6.2278 | 5.6766 | 5.4826 | 5.6777 | 6.2296 | 7.0082 | 7.7285 | 8.0284 |
| Difference | 0.0007 | 0.001 | 0.0012 | 0.0011 | 0.0012 | 0.0013 | 0.0015 | 0.0011 | 0.001 | 0.0007 | 0.0004 |

The wall shear stress (skin friction) is defined and obtained as given below:

$$\tau_w=\tau|_{r=R}=\frac{R}{2}q(z)=4\left(\frac{Qk}{R^3}\right)+32\sqrt{\frac{Qk\tau_y}{R^5}}+\frac{383}{147}\tau_y-16\sqrt{\frac{R\tau_y^3}{Qk}}. \quad (19)$$

The frictional resistance to flow is defined as

$$\lambda=\int_0^L\frac{q(z)}{Q}dz=A\int_0^L\frac{dz}{R^3}+B\int_0^L\frac{dz}{\sqrt{R^5}}+C\int_0^L R\,dz+D\int_0^L dz \quad (20)$$

where

$$A=4Qk;\ B=32\sqrt{Qk\tau_y};\ C=-16\sqrt{\frac{RQ\tau_y^3}{k}};\ D=\frac{383}{147}\tau_y. \quad (21)$$

Since the arterial segment under study has abnormal segments (stenosis and dilatation) as depicted in Figure-1(a) and as mathematically represented in Equation (6a), Equation (20) can be re-written as below:

$$\lambda=\int_0^L\frac{q(z)}{Q}dz=A\left[\int_0^{\alpha_1}\frac{dz}{R^3}+\int_{\alpha_1}^{\beta_1}\frac{dz}{R^3}+\int_{\beta_1}^{\alpha_2}\frac{dz}{R^3}++\int_{\alpha_2}^{\beta_2}\frac{dz}{R^3}+\int_{\beta_2}^{L}\frac{dz}{R^3}\right]$$
$$+B\left[\int_0^{\alpha_1}\frac{dz}{\sqrt{R^5}}+\int_{\alpha_1}^{\beta_1}\frac{dz}{\sqrt{R^5}}+\int_{\beta_1}^{\alpha_2}\frac{dz}{\sqrt{R^5}}++\int_{\alpha_2}^{\beta_2}\frac{dz}{\sqrt{R^5}}+\int_{\beta_2}^{L}\frac{dz}{\sqrt{R^5}}\right]$$
$$+C\left[\int_0^{\alpha_1}R\,dz+\int_{\alpha_1}^{\beta_1}R\,dz+\int_{\beta_1}^{\alpha_2}R\,dz++\int_{\alpha_2}^{\beta_2}R\,dz+\int_{\beta_2}^{L}R\,dz\right]+DL \quad (21)$$

On simplifying Equation (21), we get the expression for resistance to flow as Equation (22). The integrals in Equation (22) are evaluated numerically using Quadrature formula. It is noted that when $\tau_y = 0$, the expressions obtained in this paper for the flow quantities reduces to that of Newtonian fluid which are in good agreement with the corresponding expressions obtained from Priyadharshini and Ponnalagusamy [35] when $\tau_y = 0$ and $n = 1$.

$$\lambda = A\left[-\frac{1}{2\zeta}\left\{\frac{1}{(1-\zeta\alpha_1)^2}+\frac{1}{(1-\zeta\alpha_2)^2}-\frac{1}{(1-\zeta\beta_1)^2}+\frac{1}{(1-\zeta L)^2}-\frac{1}{(1-\zeta\beta_2)^2}\right\}+\int_{\alpha_1}^{\beta_1}\frac{dz}{R^3}+\int_{\alpha_2}^{\beta_2}\frac{dz}{R^3}\right]$$

$$+B\left[-\frac{2}{3\zeta}\left\{\frac{1}{(1-\zeta\alpha_1)^{3/2}}+\frac{1}{(1-\zeta\alpha_2)^{3/2}}-\frac{1}{(1-\zeta\beta_1)^{3/2}}+\frac{1}{(1-\zeta L)^{3/2}}-\frac{1}{(1-\zeta\beta_2)^{3/2}}\right\}+\int_{\alpha_1}^{\beta_1}\frac{dz}{\sqrt{R^5}}+\int_{\alpha_2}^{\beta_2}\frac{dz}{\sqrt{R^5}}\right]$$

$$+\frac{C}{2}\left[\alpha_1(2-\zeta\alpha_1)+\alpha_2(2-\zeta\alpha_2)-\beta_1(2-\zeta\beta_1)+L(2-\zeta L)-\beta_2(2-\zeta\beta_2)+\int_{\alpha_1}^{\beta_1}R\,dz+\int_{\alpha_2}^{\beta_2}R\,dz\right]+DL \tag{22}$$

## RESULTS AND DISCUSSIONS

The objective of this theoretical analysis is to study the influence of the physical parameters such as the maximum depth of stenosis $\delta_1$ and maximum height of dilatation $\delta_2$, consistency index $k$, yield stress $\tau_y$, flow rate $Q$ and angle of tapering $\psi$on the physiologically important flow quantities such as the pressure gradient, velocity profile, shear stress at the artery wall and frictional resistance to flow. To analyze the results obtained in this study and also to validate the present study with the published results of others, therange of values used for the parameters in this study are summarized below[22, 35].

Consistency index $k$ : 1 - 1.6; Maximum depth of the stenoses $\delta_1$ : 0 - 0.2; Maximum height of dilatation $\delta_2$: $-0.2 - 0$; Angle of tapering $\psi$: $-0.02 - 0.02$; Flow rate $Q$: 1 – 2; Yield stress: $\tau_y$ : $0 - 0.2$.

### Pressure gradient

The axial variation in the pressure gradient for different values of angle of tapering $\psi$ and yield stress $\tau_y$ with $k$ = 1.2, $Q$ = 1, $\delta_1 = 0.2$ and $\delta_2 = -0.2$ is depicted in Figure-2. For a given set of values of the parameters, the pressure gradient soars (nonlinearly) with the increase of the axial variable from $z$ = 2 to $z$ = 2.5 (with the increase of the stenosis depth from 0 to 0.2) and then it slumps (nonlinearly) with increase of the axial variable from $z$ = 2.5 to $z$ = 3 (with the decrease of the stenosis depth from 0.2 to 0) and it decreases very slightly with the increase of the is almost constant with the increase of the axial variable from $z$ = 3 to $z$ = 4 (in the non-stenotic tapered region) and it decreases significantly with the increase of the axial variable from $z$ = 4 to $z$ = 4.5 (with the increase of the dilatation height from 0 to 0.2) and it increases rapidly with the increase of the axial variable from $z$ = 4.5 to $z$ = 5 (with the decrease of the dilatation height from 0.2 to 0).One can also observe that the pressure gradient increases considerably with the increase of the yield stress $\tau_y$ when the angle of tapering is fixed and it decreases marginally with the increase of the angle of tapering $\psi$ of the artery while the yield stress $\tau_y$ is held constant.

The variation of pressure gradient in the axial direction for different values of $Q$, $k$, $\delta_1$ and $\delta_2$ with $\psi = 0^\circ$ and $\tau_y = 0.1$ is delineated in Figure-3. For a given set of values of parameters $Q$ and $k$, the pressure gradient in blood increases significantly with the increase of the stenosis depth and it decreases significantly with the increase of the dilatation height. It is also clear that the pressure gradient in blood flow increases considerably with the increase of the consistency index $k$ while the rest of the parameters are held constant. Once can also observe that the pressure gradient in blood flow increases very significantly with the increase of the flow rate $Q$ when all the other parameters kept as invariables. Figures 2 and 3 brings out the effect of the parameters $Q, k, \tau_y, \delta_1, \delta_2$ and $\psi$ on the pressure gradient in blood flow through narrow tapered arteries with constriction and dilatation.

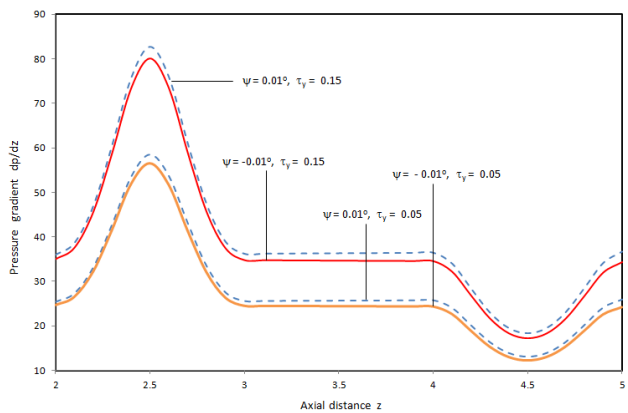


**Figure-2.** Axial variation in pressure gradient for various values of $\psi$ and $\tau_y$ with $k$ = 1.2 and $\delta_1 = 0.2$ and $\delta_2 = -0.2$ .

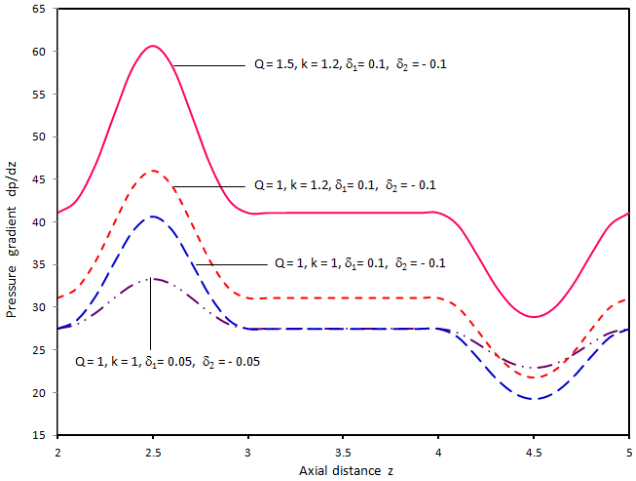


**Figure-3.** Axial variation in pressure gradient for different values of $Q$, $k$, $\delta_1$ and $\delta_2$ with $\psi = 0^o$ and $\tau_y = 0.1$.

**Velocity profile**

The velocity profiles of blood flow for different values of the consistency index k and yield stress $\tau_y$ with $Q = 1$, $\delta_1 = 0.1$, $\delta_2 = -0.1$ and $\psi = 0^o$ are sketched in Figure-4. One can notice the flattened parabolic velocity profile of blood as expected for non-Newtonian fluids with yield stress. For a given set of values of the parameters $Q$, $\delta_1$, $\delta_2$ and $\psi$, the blood velocity decreases considerably with the increase of the yield stress $\tau_y$ of blood and it decreases significantly with the increase of the consistency index $k$. The velocity profiles of blood at different locations of stenos is and dilatation in the axial direction with $k = Q = 1$, $\tau_y = \delta_1 = 0.1$, $\delta_2 = -0.1$ and $\psi = 0.01^o$ are illustrated in Figure-5. It is clear that the blood velocity decreases with the increase of the stenosis depth and an opposite behavior is noted when the dilatation height increases.

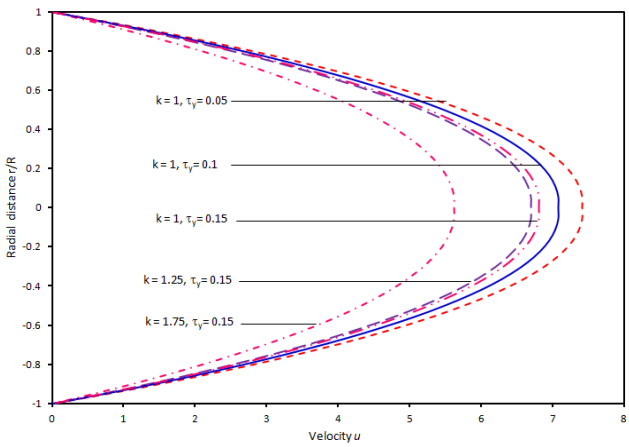


**Figure-4.** Velocity profile for different values of $k$ and $\tau_y$ with $Q = 1$, $\delta_1 = 0.1$, $\delta_2 = -0.1$ and $\psi = 0^o$.

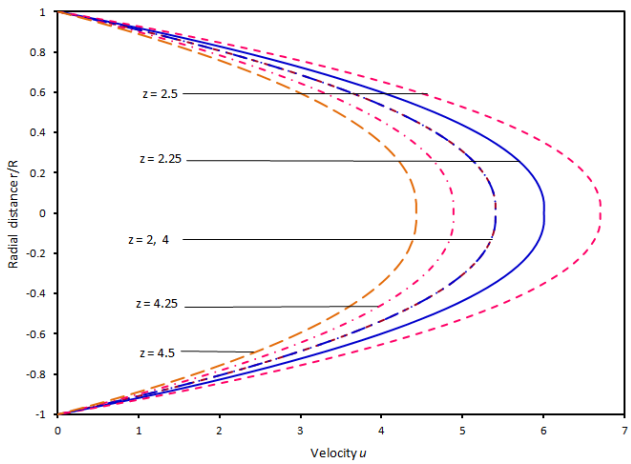


**Figure-5.** Velocity profiles at different locations in the axial direction with $k = Q = 1$, $\delta_2 = -0.1$, $\tau_y = \delta_1 = 0.1$ and $\psi = 0.01^o$.

**Wall shear stress distribution**

It has been well accepted that the wall shear stress plays a vital role in the endothelial homeostasis and the focal distribution of atherosclerotic lesions [36 - 38]. The axial variation in wall shear stress for different values of angle of tapering $\psi$ and maximum depth of stenosis $\delta_1$ and maximum height of dilatation $\delta_2$ with $k = Q = 1$ and $\tau_y = 0.1$ is shown in Figure-6. It is observed that the wall shear stress increases rapidly (nonlinearly) with the increase of the axial variable from $z = 2$ to $z = 2.5$ and then it decreases drastically (nonlinearly) with increase of the axial variable from $z = 2.5$ to $z = 3$ and is almost constant with the increase of the axial variable from $z = 3$ to $z = 4$ (in the non-stenotic tapered region) and it falls heavily with the increase of the axial variable from $z = 4$ to $z = 4.5$ and it rises rapidly with the increase of the axial variable from $z = 4.5$ to $z = 5$. For a given set of values of the parameters $k$, $Q$ and $\tau_y$, the wall shear stress decreases marginally with the increase of angle of tapering of the artery $\psi$. It is also noticed that the wall shear stress increases significantly with the increase of the maximum height of stenosis and it decreases considerably with the increase the dilation height.

Figure-7 delineates the variation of wall shear stress in the axial direction for different values of the consistency index $k$ and yield stress $\tau_y$ with $\psi = 0$, $\delta_1 = 0.1$ and $\delta_2 = -0.1$ and $Q = 1$. It is found that the wall shear stress in the blood flow increases significantly with the increase of the yield stress $\tau_y$ of blood when all the other parameters kept as invariables. For fixed value of yield stress $\tau_y$, the wall shear stress increases considerably when the consistency index of blood increases. It is of important to note that the plot of Newtonian fluid's wall shear stress is in good agreement with the corresponding plot in Figure-4 of Priyadharshini and Ponnalagu Samy

[35]. Figures-6 and 7 spell out the influence of the parameters yield stress, angle of tapering, stenosis depth, dilatation height and consistency index on the wall shear stress in blood flow through narrow arteries.

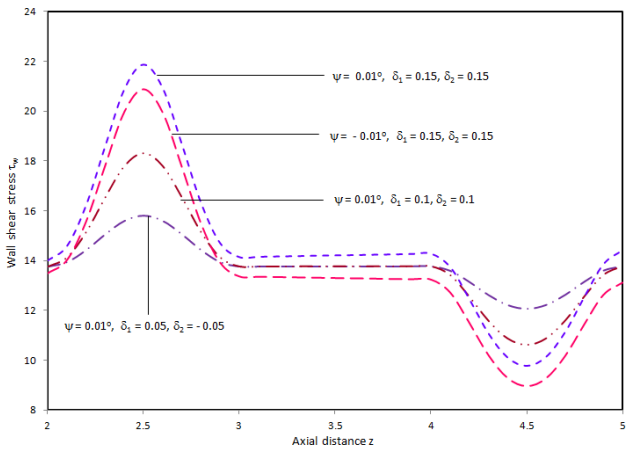


**Figure-6.** Axial variation in wall shear stress for different values of $\psi$, $\delta_1$ and $\delta_2$ with $k = Q = 1$, $\tau_y = 0.1$.

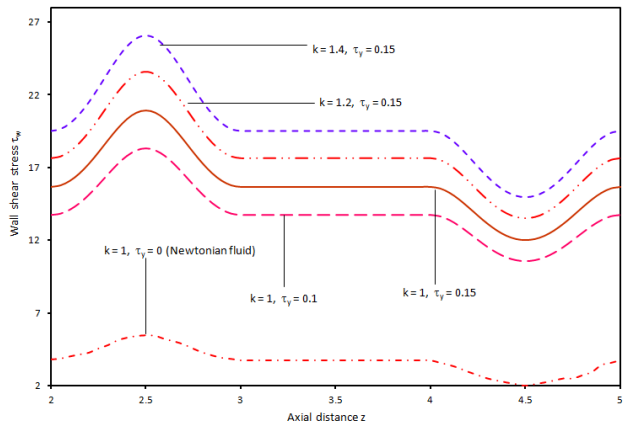


**Figure-7.** Axial variation in wall shear stress for different values of $k$ and $\tau_y$ with $\psi = 0$, $\delta_1 = 0.1$ and $\delta_2 = -0.1$ and $Q = 1$.

## Frictional resistance to flow

Frictional resistance to flow is an important rheological measurement in the investigation of blood flow through arteries in the abnormal state, like constriction, dilation, catheterization etc. Figure-8 shows the axial variation in frictional resistance to flow for different values of consistency index $k$ and angle of tapering $\psi$ with $\tau_y = \delta_1 = 0.1$, $\delta_2 = -0.1$ and $Q = 1$. For a given value of the consistency index $k$, the frictional resistance in blood flow increases slightly with the increase of the angle of tapering (i.e. when the artery narrows in diameter) and it increases considerably with the increase of the consistency index $k$ while rest of the parameters held constant. The variation of frictional resistance to blood flow with axial distance for various values of flow rate $Q$ and yield stress $\tau_y$ with $\psi = 0.01$, $\delta_1 = 0.1$ and $\delta_2 = -0.1$ and $k = 1$ is depicted in Figure-9. One can notice that the frictional resistance to flow increases rapidly when the yield stress $\tau_y$ of blood increases and the flow rate $Q$ is constant, whereas an opposite behavior is observed when the flow rate $Q$ increases and the yield stress $\tau_y$ of blood is treated as invariable. Figures 8 and 9 propounded the influence of the parameters consistency index, angle of tapering, flow rate and yield stress on frictional resistance to blood flow through narrow arteries with constriction and dilation.

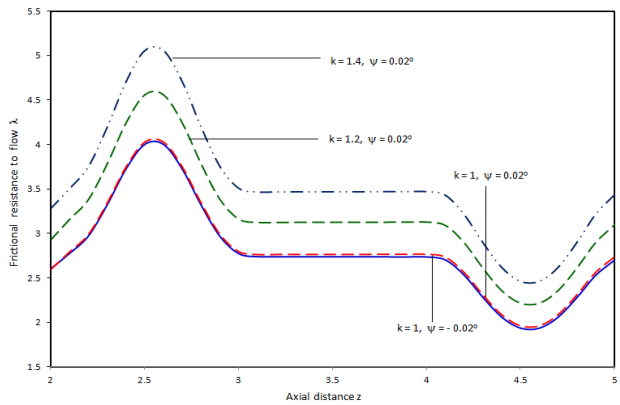


**Figure-8.** Axial variation in longitudinal impedance to flow for different values of $k$ and $\psi$ with $\delta_1 = 0.1$, $\delta_2 = -0.1$ and $Q = 1$.

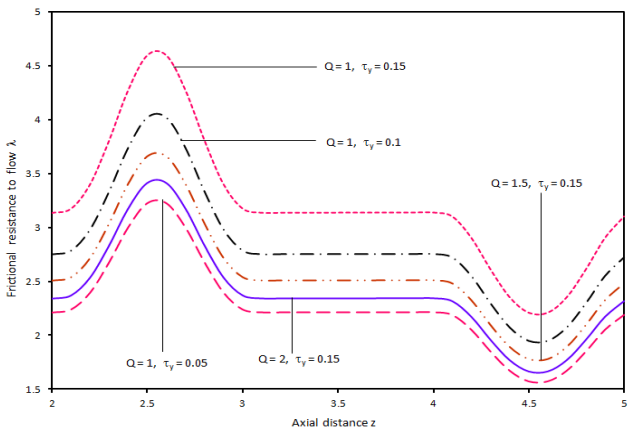


**Figure-9.** Axial variation in longitudinal impedance to flow for $Q$ and $\tau_y$ with $\psi = 0.01$, $\delta_1 = 0.1$ and $\delta_2 = -0.1$ and $k = 1$.

The percentage of increase in the frictional resistance to flow due to the increase in the maximum depth of stenosis $\delta_1$ and yield stress $\tau_y$ with $z = 2.5$, $k = Q = 1$ and $\psi = 0.01°$ is computed in Table-3. It is found that the percentage of increase in the frictional resistance to flow increases rapidly (nonlinearly) with the increase of the maximum depth of stenosis and it increases marginally

with the increase of the yield stress $\tau_y$ of blood. Note that in the case of Newtonian fluid flow, these increases are 20.23, 46.05, 79.13, 122.27 and 179.64 when the values of the maximum depth of stenosis $\delta_1$ are 0.05, 0.1, 0.15 and 0.2 respectively. Table-4 computes the percentage of increase in the frictional resistance to flow due to the increase in the maximum height dilatation $\delta_2$ and yield stress $\tau_y$ with $z = 2.5$, $k = Q = 1$ and $\psi = 0.01°$. One can observe that the percentage of increase in the frictional resistance to flow increases significantly with the increase of the maximum depth of stenosis and it increases slowly with the increase of the yield stress $\tau_y$ of blood.

**Table-3.** Percentage of increase in frictional resistance to flow due to the increase in the maximum depth of stenosis $\delta_1$ and yield stress $\tau_y$ with $z = 2.5$, $k = Q = 1$ and $\psi = 0.01°$.

| $\delta_1$ \ $\tau_y$ | 0 | 0.05 | 0.1 | 0.15 | 0.2 |
|---|---|---|---|---|---|
| 0.05 | 20.23 | 20.25 | 20.51 | 20.81 | 21.95 |
| 0.1 | 46.05 | 46.15 | 46.53 | 47.18 | 50.26 |
| 0.15 | 79.13 | 79.17 | 79.92 | 81.03 | 87.3 |
| 0.2 | 122.3 | 122.53 | 123.42 | 125.01 | 136.51 |
| 0.25 | 179.6 | 180.18 | 181 | 183.36 | 203.03 |

**Table-4.** Percentage of increase in frictional resistance to flow due to the increase in the height of dilatation $\delta_2$ and yield stress $\tau_y$ with $z = 4.5$, $k = Q = 1$ and $\psi = 0.01°$.

| $\delta_2$ \ $\tau_y$ | 0 | 0.05 | 0.1 | 0.15 | 0.2 |
|---|---|---|---|---|---|
| - 0.05 | 16.11 | 16.2 | 16.38 | 16.62 | 17.22 |
| - 0.1 | 29.07 | 29.24 | 29.59 | 30.02 | 26.17 |
| - 0.15 | 39.6 | 39.86 | 40.34 | 40.93 | 41.17 |
| - 0.2 | 48.24 | 48.6 | 49.18 | 49.9 | 50.71 |
| - 0.25 | 55.38 | 55.8 | 56.49 | 57.32 | 57.94 |

**Streamlines**

The streamlines of the blood flow pattern for the yield stress values $\tau_y = 0$, $\tau_y = 0.15$, $\tau_y = 0.05$ and $\tau_y = 0.1$ are illustrated in Figures 10(a), 10(b), 10(c) and 10(d) respectively. One can visualize the widening of the plug flow region around the axis of the artery when the yield stress of blood increases. It is of interest to note that the streamlines of Newtonian fluid flow (when $\tau_y = 0$) is in good agreement with the corresponding plot in Figure-14(a) of Priyadharshini and Ponnalagu Samy [35]. From the streamlines, one can easily observe the considerable changes in the in the direction of flow in the constriction (stenosis) region and dilatation region. Figure-11(a) - 11(d) depicts the streamlines pattern in blood flow for the consistency index $k$ values 0.75, 1, 1.25 and 1.5 respectively. It is seen that the increase in the consistency index value increases the width of the plug flow region. The streamlines pattern in blood flow for the flow rate $Q$ values 0.75, 1, 1.5 and 2 are sketched in Figures 12(a) - 12(d) respectively. These plots indicate that the increase of the flow rate enhances the volume of fluid passing the around the artery axis where maximum velocity occurs. Figures 13(a) - 13(d) delineates the streamlines of blood flow when (a) $\delta_1 = 0, \delta_2 = 0$; (b) $\delta_1 = 0.05, \delta_2 = -0.05$; (c) $\delta_1 = 0.1, \delta_2 = -0.1$ and (d) $\delta_1 = 0.1, \delta_2 = -0.1$ respectively. One can clearly see the changes in streamline pattern in the stenos is and dilation region due to the increase in the maximum depth of stenos is and maximum height of dilation.

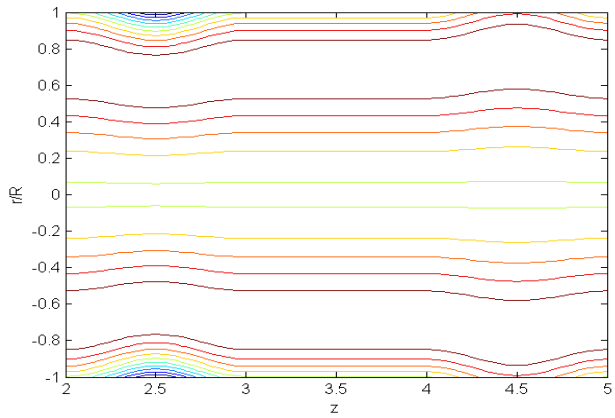


(a) $\tau_y = 0$.

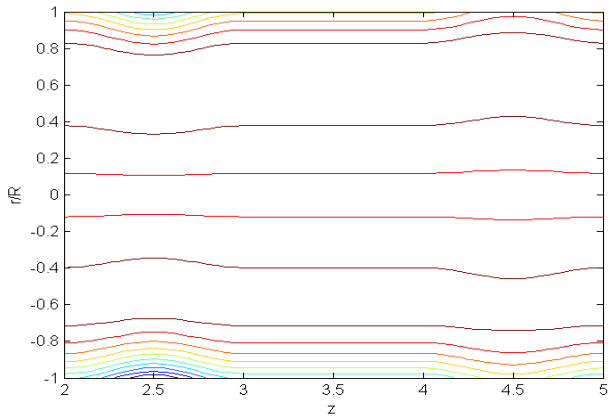


(b) $\tau_y = 0.05$.

VOL. 13, NO. 17, SEPTEMBER 2018 ISSN 1819-6608
ARPN Journal of Engineering and Applied Sciences



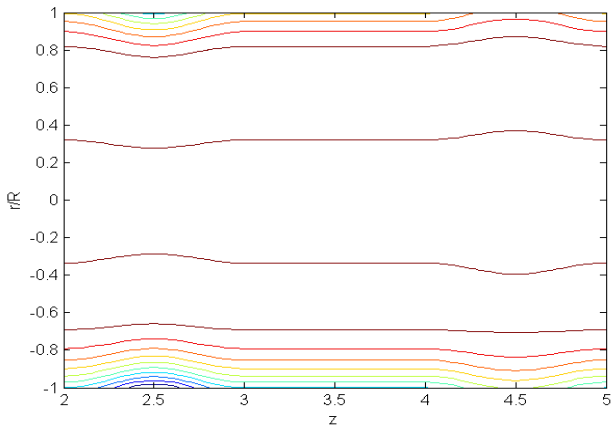


(c) $\tau_y = 0.1$.

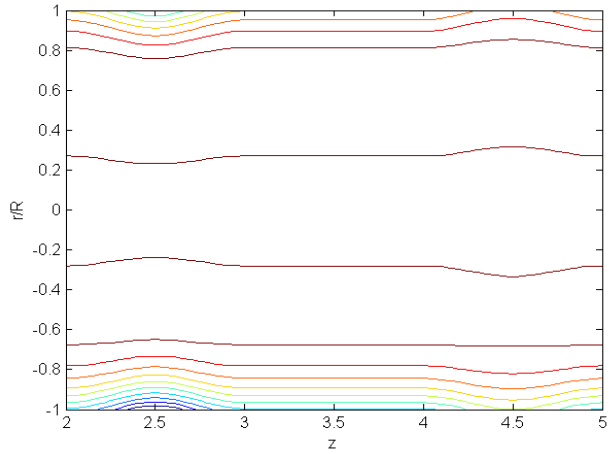


(d) $\tau_y = 0.15$.

**Figure-10.** Stream lines pattern of the flow field for different values of yield stress $\tau_y$ with $\psi = 0.01$, $\delta_1 = \delta_2 = 0.1$ and $k = Q = 1$.

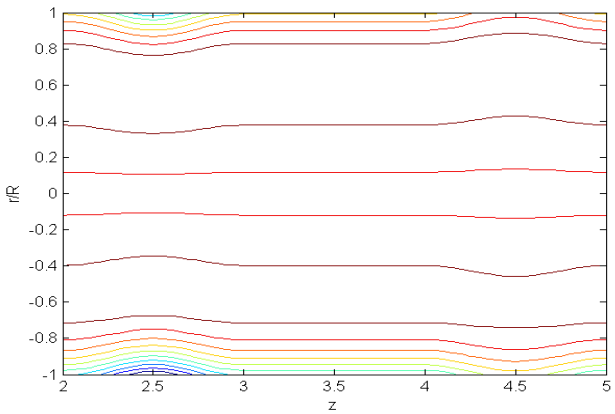


(a) $k = 0.75$.

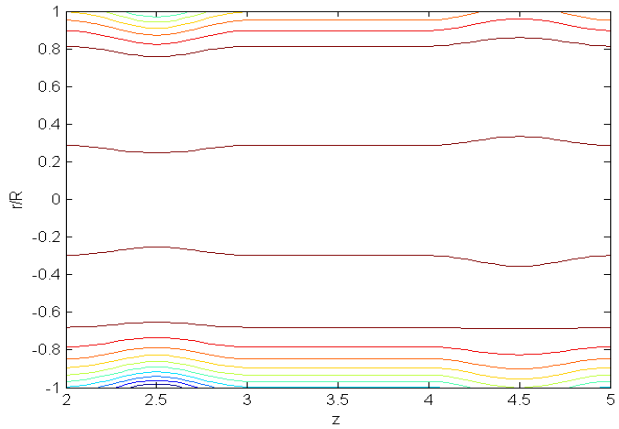


(b) $k = 1$.

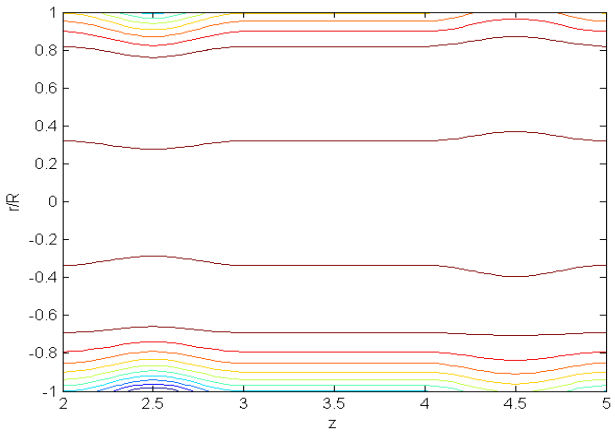


(c) $k = 1.25$.

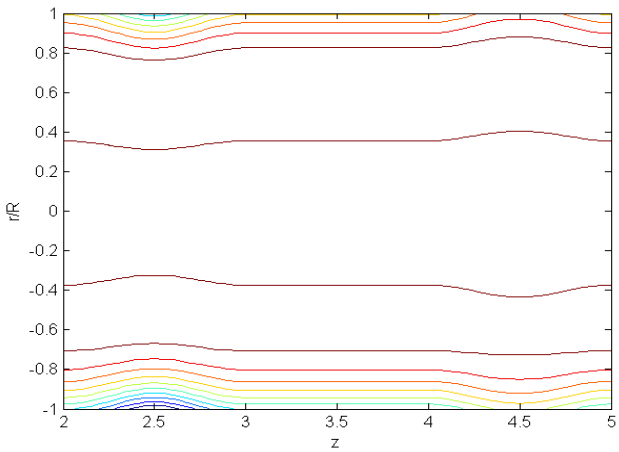


(d) $k = 1.5$.

**Figure-11.** Stream lines pattern of the flow field for different values of consistency index $k$ with $\tau_y = \delta_1 = \delta_2 = 0.1$, $\psi = 0.01$ and $k = Q = 1$.

VOL. 13, NO. 17, SEPTEMBER 2018 ISSN 1819-6608
ARPN Journal of Engineering and Applied Sciences



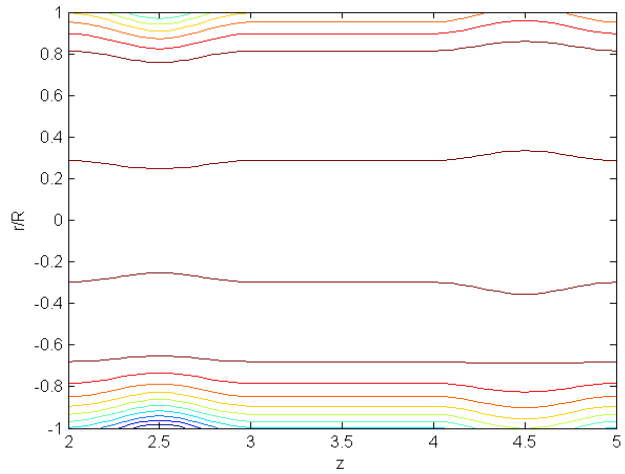


(a) Q = 0.75.

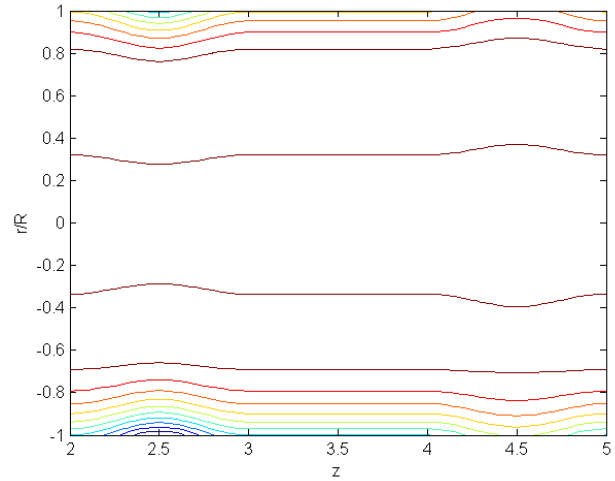


(b) Q = 1.

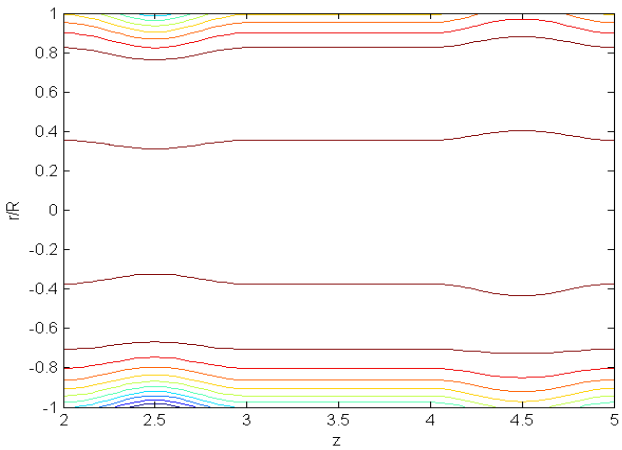


(c) Q = 1.5.

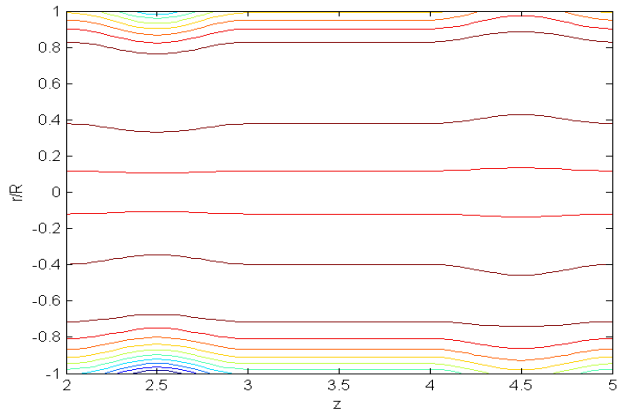


(d) Q = 2.

**Figure-12.** Stream lines pattern of the flow field for different values of flow rate $Q$ with $\tau_y = \delta_1 = \delta_2 = 0.1$, $\psi = 0.01$ and $k = 1$.

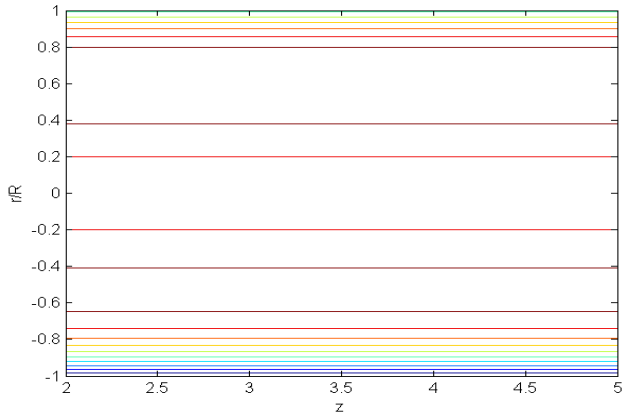


(a) $\delta_1 = \delta_2 = 0$.

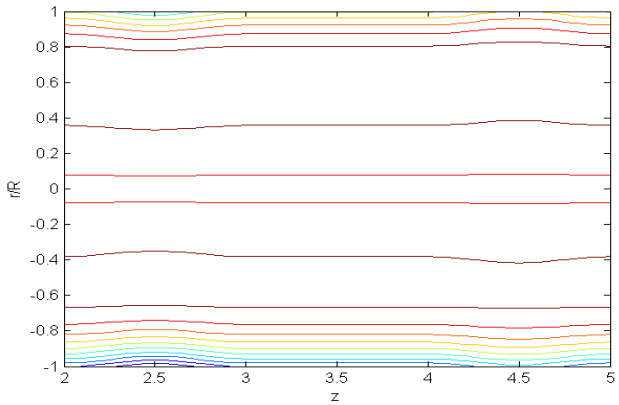


(b) $\delta_1 = 0.05,\ \delta_2 = -0.05$.

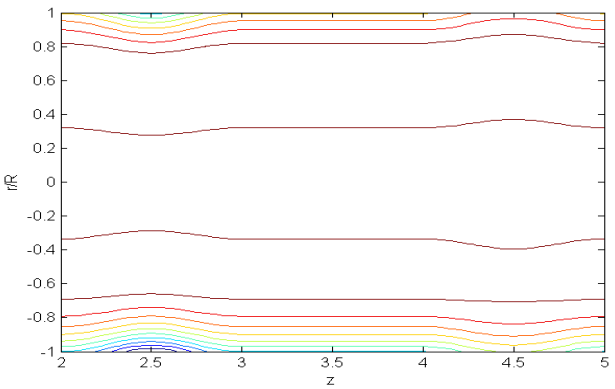


(c) $\delta_1 = 0.1,\ \delta_2 = -0.1$

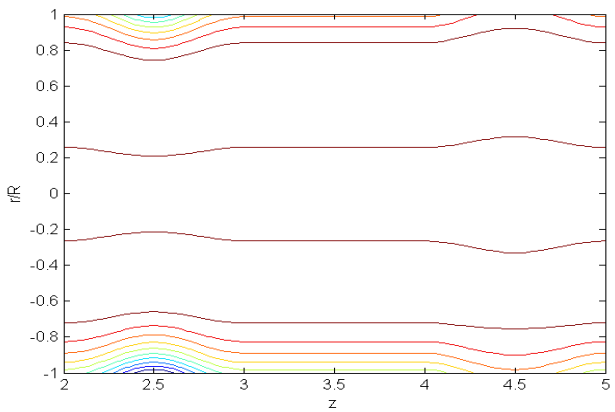


(d) $\delta_1 = 0.15,\ \delta_2 = -0.15$.

**Figure-13.** Stream lines pattern of the flow field for different values of stenosis depth $\delta_1$ and dilatation height $\delta_2$ with $\tau_y = 0.1$, $\psi = 0.01$ and $k = Q = 1$.

## CONCLUSIONS

This mathematical investigation brings out several useful rheological characteristics of blood when it flows in a tapered narrow artery with mild axi-symmetric stenosis and dilatation. Blood is represented by non-Newtonian Casson fluid and the flow is considered as steady, axi-symmetric, laminar, fully developed and uni-directional in the axial direction. The influence of various rheological parameters on the physiologically useful flow quantities is discussed. The major findings of this mathematical analysis are listed below:

- The pressure gradient increases considerably with the increase of the yield stress $\tau_y$ and consistency index $k$ of blood and, it decreases marginally with the increase of the angle of tapering $\psi$ of the artery.
- The pressure gradient increases significantly with the increase of the stenosis depth $\delta_1$ and flow rate $Q$ and, it decreases significantly with the increase of the dilatation height.
- The blood velocity decreases considerably with the increase of the yield stress $\tau_y$ of blood and it decreases significantly with the increase of the consistency index $k$.
- The wall shear stress decreases considerably with the increase of angle of tapering $\psi$ of the artery, maximum height of stenosis $\delta_1$, consistency index $k$ and yield stress $\tau_y$ of blood and, it decreases considerably with the increase the dilatation height.
- The frictional resistance in blood flow increases slightly with the increase of the angle of tapering and it increases considerably with the increase of the consistency index $k$.
- The frictional resistance to flow increases rapidly when the yield stress $\tau_y$ of blood increases, but an opposite behavior is found when the flow rate $Q$ increases.
- The percentage of increase in the frictional resistance to flow increases rapidly with the increase of the maximum depth of stenosis and maximum height of dilatation and, it increases marginally with the increase of the yield stress $\tau_y$ of blood.

The results of this mathematical analysis bring out several salient features which may be useful to the clinicians and medical surgeons in analyzing the consequences of the constrictions and protuberance that are developed in the lumen of the artery. Hence, it is concluded that the present study may be considered as advancement in the mathematical analysis of blood flow in tapered narrow blood vessels with constriction and dilatation. Since, the pulsatile flow of blood flow is more realistic in nature, the pulsatile flow of blood in tapered artery with different geometries of constrictions and dilations in the presence of magnetic field and body acceleration would be studied in the near future.

## REFERENCES

[1] Pincombe B. & MazumdarJ.Craig I. H. 1999. Effects of multiple stenoses and post-stenotic dilatation on non-Newtonian blood flow in small arteries. Med. Biol. Engg. Comput. 37: 595-599.

[2] Ismail Z, Abdullah I., Mustapha N. & Amin N. 2008. A power law model of blood flow through a tapered overlapping stenosed artery. Appl. Math. Computat. 195: 669-680.

[3] Siddiqui A. 2011. Effects of vasodilation and arterial resistance on cardiac output. J Clinic Experiment Cardiol. 2(11): Article ID. 1000170.

[4] Nadeem S., Akbar N. S., Hendi A. A. & Hayat T. 2011. Power law fluid model for blood flow through a tapered artery with a stenosis. Appl. Math. Computat. 217: 7108-7116.

[5] Biswas D. & Laskar R. B. 2011. Steady flow of blood through a stenosed artery-A non-Newtonian fluid model. Assam University J. Sci. and Tech. 7: 144-153.

[6] Ponalagusamy R. 2012. Mathematical analysis on effect of non-Newtonian behavior of blood on optimal geometry of microvascular bifurcation system. J. Franklin Institute. 349: 2861-2874.

[7] Venkatesan J, Sankar D. S.,Hemalatha K. & Yazariah Y. 2013. Mathematical analysis of Casson fluid model for blood rheology in stenosed narrow arteries. J. Appl. Math. Article ID: 583809.

[8] Sarifuddin S. 2014. Simulation of Casson fluid flow and heat transport in differently shaped stenosis. J. Mech. Mech. Biol. 14: Article ID: 1450024.

[9] Mekheimer Kh. S. & El KotM. A. 2012. Mathematical modeling of unsteady flow of Sisko fluid through an anisotropically tapered elastic arteries with time-variant overlapping stenosis. App. Math. Model. 36: 5393-5407.

[10] Karimpour H. &Javdan E. 2014.Simluation of stenosis growth in the carotid artery by Lattice Boltzmann method. J. Mech. Med. Biol. 14: Article ID: 1450016.

[11] Chang W. Y., Ding Y. &TuJ. Y. 2007. Modeling of non-Newtonian blood flow through a stenosed artery incorporating fluid structure interaction. Australia and New Zealand J. Appl. Math. 47: 507-523.

[12] Tang D., Tang C., Kobayashi S. & Ku D. N. 2001. Generalized finite difference method for 3D viscous flow in stenotic tubes with large wall deformation and collapse. Appl. Num. Math. 38: 49-68.

[13] Guo, X,Razandi M,Pedram A., Kassab G. & Levin E. R. 2005. Estrogen Induces Vascular Wall Dilation: Mediation through kinase signaling to nitric oxide and estrogen receptors $\alpha$ and $\beta$ .J. Biol. Chem. 280: 19704–19710.

[14] Alvarez E., Cairrão E., Morgado M., Morais, C &Verde I. Testosterone and cholesterol vasodilation of rat aorta involves L-type calcium channel inhibition. Adv. Pharmacol. Sci. Vol. 2010: Article ID: 534184.

[15] Guntheroth W. G. 2010. Increased Pulse Pressure Causes Vascular Injury in Pulmonary and Systemic Arteries: Decreasing the Pulsatility with Banding and Vasodilators Can Stabilize Pulmonary Hypertension. J. Clinic Experiment Cardiol. 1: 107.

[16] Kirby B. S., Crecelius, A. R., Voyles W. F. & Dinenno F. A. 2010. Vasodilatory responsiveness to adenosine tri-phosphate in ageing humans. J. Physiol. 588: 4017-4027.

[17] Citterio L., Simonini M., Zagato L., Slave E. & Carline S. D. Genes involved in vasoconstriction and vasodilation system affect salt-sensitive hypertension. PLoS One. 6: 19620.

[18] Tanaka Y., Matsuo K. & Yuzuriha S. 2011. Near-Infrared Irradiation Nonthermally Induces Long-lasting Vasodilation by Causing Apoptosis of Vascular Smooth Muscle Cells. Eplasty 11: 22.

[19] Srivastava V. P., Arterial blood flow through a nonsymmetrical stenosis with applications. Japanese Journal of Applied Physics. 34(12): 6539-6545.

[20] Ponalagusamy R., Tamil Selvi R. & Banerjee A. K. 2012. Mathematical model of pulsatile flow of non-Newtonian fluid in tubes of varying cross-sections and its implications to blood flow. J. Franklin Institute. 349: 1681-1698.

[21] Akbar N. S. & Nadeem S. 2014. Carreau fluid model for blood flow through a tapered artery with a stenosis. Ain Shams Engng. J. 5: 1307-1316.

[22] Nagarani P. & Sarojamma G. 2008. Effect of body acceleration on pulsatile flow of Casson fluid through a mild stenosed artery. Korea-Australia Rheol J. 20: 189-196.

[23] JonhstonB. M., Johmston P.R., Corney S. & Kilpatrick D. 2004. Non-Newtonian blood flow in human right coronary arteries steady state simulations. J. Biomech. 37: 709-720.

[24] Sankar D. S. & Hemalatha K. 2007. Pulsatile flow of Herschel-Bulkley fluid through catheterized arteries-A mathematical model. Appl. Math. Model. 31: 1497-1517.

[25] Husna T., Abdul Rahman T., Salma U. K. & Ahmad D. R. 2016. Mathematical model of carotid artery for stent placement.AIP Conf. Proceed.1784: Article ID: 050019.

[26] Chaturani P & Ponalagusamy R. 1986. Pulsatile flow of Casson's fluid through stenosed arteries with applications to blood flow. Biorheology. 23: 499-511.

[27] Casson N. 1959. In: Rheology of disperse systems (Edited by Mill, C.C). Pergamon Press, London.

[28] Scott Blair G. W. 1959. An Equation for the Flow of Blood, Plasma and Serum through Glass Capillaries. Nature. 183: 613.

[29] Merrill E. W.,Benis A. M., Gilliland A. R., Sherwood T. K. & Salzman E. W. 1965. Pressure flow relations of human blood in hollow fibers at low shear rates. J. Appl. Physiol. 20: 954-967.

[30] Scott Blair G. W. & Spanner D. C. 1974. An introduction to Biorheology, Elsevier Scient. Publ. Co., Amsterdam, Oxford and New York.

[31] Srivastava V. P. & Saxena M. 1994. Two-layered model of casson fluid flow through stenotic blood vessels: applications to the cardiovascular system. J. Biomech. 27: 921-928.

[32] Sankar D. S. & Lee U. 2008. Two-fluid non-linear model for flow in catheterized blood vessels. Int. J. Non-Linear Mech. 43: 622-631.

[33] Dash R. K., Jayaraman G. & Metha K. N. Estimation of increased flow resistance in a narrow catheterized artery-A theoretical model. J. Biomech. 29: 917-930.

[34] Pincombe B. Mazumdar J. & Hamilton-Craig I. 1999. Effects of multiple stenoses and post-stenostic dilatation on non-Newtonian blood flow in small arteries. Medical & Biological Engineering & Computing: 37: 595-599.

[35] Priyadharshini S. & Ponnalagarsamy R. 2015. Biorheological model on flow of Herschel-Bulkley through a tapered arterial stenosis with dilatation. Appl. Bionics and Biomech. Vol. 2015, Article ID.: 406195.

[36] Gibson C. M., Diaz L., Kandarpa K., Sacks F. M., Pasternak R. C., Sandor T., Feldman C. & Stone P. H. 1993. Relation of vessel wall shear stress to atherosclerosis progression in human coronary arteries. Arteriosclerosis and Thrombosis. 13: 310-315.

[37] Friedman M. H., Bargeron C. B., Duncan D. D., Hutchins G. M. & Mark F. F., Effects of arterial compliance and non-Newtonian rheology on correlations between intimal thickness and wall shear. J. Biomech. Eng. 114: 317-320.

[38] Pedersen E. M, Agerbǽk M., Kristensen I. B. & Yoganathan A. P. 1997. Wall shear stress and early atherosclerotic lesions in the abdominal aorta in young adults. Eu. J. Vasc. Endovasc. Surg. 13: 443-451.